Climate Dynamics (2001) 17: 277–289

R. Wu · B. Wang

Multi-stage onset of the summer monsoon over the western North Pacific*

Received: 19 October 1999 / Accepted: 5 June 2000

Abstract The climatological summer monsoon onset displays a distinct step wise northeastward movement over the South China Sea and the western North Pacific (WNP) (110°–160°E, 10°–20°N). Monsoon rain commences over the South China Sea-Philippines region in mid-May, extends abruptly to the southwestern Philippine Sea in early to mid-June, and finally penetrates to the northeastern part of the domain around mid-July. In association, three abrupt changes are identified in the atmospheric circulation. Specifically, the WNP subtropical high displays a sudden eastward retreat or quick northward displacement and the monsoon trough pushes abruptly eastward or northeastward at the onset of the three stages. The step wise movement of the onset results from the slow northeastward seasonal evolution of large-scale circulation and the phase-locked intraseasonal oscillation (ISO). The seasonal evolution establishes a large-scale background for the development of convection and the ISO triggers deep convection. The ISO over the WNP has a dominant period of about 20–30 days. This determines up the time interval between the consecutive stages of the monsoon onset. From the atmospheric perspective, the seasonal sea surface temperature (SST) change in the WNP plays a critical role in the northeastward advance of the onset. The seasonal northeastward march of the warmest SST tongue (SST exceeding 29.5 °C) favors the northeastward movement of the monsoon trough and the high convective instability region. The seasonal SST change, in turn, is affected by the monsoon through cloud-radiation and wind-evaporation feedbacks.

* This paper is a contribution to the AMIP-CMIP Diagnostic Subproject on General Circulation Model Simulation of the East Asian Climate (EAC). Coordinated by W.-C. Wang.

R. Wu · B. Wang (✉)
Department of Meteorology and International Pacific Research Center, School of Ocean and Earth Science and Technology, University of Hawaii at Manoa, Honolulu, HI 96822, USA
E-mail: bwang@soest.hawaii.edu

1 Introduction

The western North Pacific (WNP) is a distinct monsoon region (Murakami et al. 1992; Wang 1994). In the mature phase of the WNP summer monsoon (WNPSM), the convection over the WNP becomes as strong as that over the Indian monsoon region (Murakami and Matsumoto 1994). Due to the release of large amounts of latent heat, the WNP becomes a major heating center in the upper troposphere in summer (Yanai and Tomita 1998). The upper-level divergent flow from the WNP to the eastern tropical Pacific is of particular relevance to the El Niño-Southern Oscillation (ENSO) (Rasmusson and Arkin 1987). The convective activity over the WNP has considerable influence on the weather and climate in the East Asia (Nitta 1987). Wang et al. (1999) pointed out that the Philippine Sea pressure and wind anomalies play a key role for linking ENSO to the East Asian climate.

The onset of the summer monsoon is the most significant phenomenon in the subseasonal variation of the monsoon. The onset reflects the start of rainy season and frequent convective activity, accompanied by dramatic changes of large-scale atmospheric circulation. The monsoon rain onset is critical for local agriculture in continental Asia. Over the ocean, the latent heat release due to deep convection affects atmospheric circulation over remote land areas and impacts on the weather and climate in crop cultivation regions.

The climatological rainy season commences in low latitudes and advances poleward. The advance, however, is not purely meridional due to the effects of land and sea distribution. Over the Bay of Bengal and the Indian subcontinent, the onset advances northwestward (Indian Meteorological Department 1943). Over Indonesia and northern Australia, the onset progresses southeastward (Murakami and Matsumoto 1994). Over the WNP, the onset displays distinct northeastward march (Wang 1994; Murakami and Matsumoto 1994). It was speculated that annually varying sea surface temperature

(SST) and SST gradients contribute to the march of the onset (Wang 1994). Murakami and Matsumoto (1994) speculated the role of the zonal SST gradient along 10°–20°N in the development of the WNPSM onset. Ueda and Yasunari (1996) suggested that the development of a warm SST tongue around 20°N and 150°E in early-July leads to an abrupt enhancement of convection in late-July. The process by which the SST variation affects such a distinct onset advance is not well understood.

The monsoon rainy onset is an abrupt phenomenon. In the South China Sea (SCS) and WNP (the WNPSM domain refers to the region of 110°–160°E, 10°–20°N in this study), the climatological rainy onset displays three distinct stages (Wu and Wang 1999). Figure 1 shows a Hovemöller diagram of the climatological pentad mean rain rate along 15°N. If we the 6 mm/day rain rate as the threshold for the monsoon rainfall, the onset in the SCS is observed around pentad 27–28 (May 11–20) as indicated by a quick increase of the rain rate from below to above 6 mm/day in the SCS. The second stage onset occurs around pentad 34 (June 15–19) in the southwestern Philippine Sea when the east bound of the 6 mm/day contour extends suddenly to around 140°E. During pentad 34–40, the eastward extension of the monsoon rain is slow with intraseasonal fluctuations. Another sudden eastward expansion of the heavy rain rate region is seen around pentad 40–41 (July 15–24), signifying the third stage onset in the northeastern part of the domain.

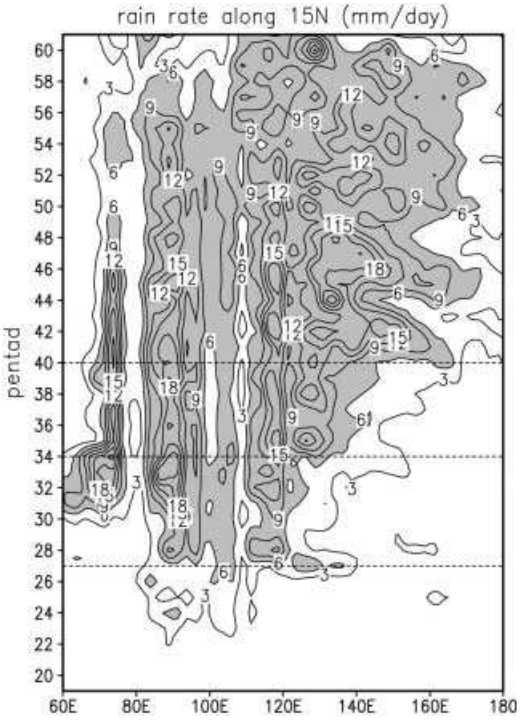

Fig. 1 Climatological pentad mean rain rate along 15°N. The contour interval is 3 mm/day. *Shading* denotes rain rate over 6 mm/day. The *dashed horizontal lines* indicate the onset time of the three stages

Why does the onset display distinct stages? This problem is not well understood. Previous studies identified the role of the intraseasonal oscillation (ISO) in the summer monsoon onset (Murakami et al. 1986; Hendon and Liebmann 1990; Chen and Chen 1995; Soman and Kumar 1993; Murakami and Matsumoto 1994; Lau et al. 1988). Tanaka (1992) indicated that the sudden northward advance of the cloud band over East Asia and the subtropical WNP are associated with the climatological ISO. Wang and Xu (1997) proposed four subseasonal cycles during May–October that link all major sudden changes in the onset using the concept of the climatological ISO. The first cycle has a wet phase in mid-May that starts the monsoon over the SCS and Philippines. The wet phase of cycle II peaking in mid-June marks the onset of the WNPSM, the continental Indian summer monsoon, and Meiyu.

The present study focuses on the formation of the multiple stages of the onset in the WNPSM domain. The objectives are to understand the causes for the step wise northeastward advance of the onset and the role of the seasonal SST change in the WNP.

2 Data

The rainfall data used in this study are from the Climate Prediction Center Merged Analysis of Precipitation (CMAP) (Xie and Arkin 1997). The climatological pentad mean CMAP rainfall was constructed based on the original pentad means from 1979 to 1996 with a global coverage on 2.5° × 2.5° grids. The OLR data are used as a proxy to represent the deep convection in the tropics with some cautions. The climatological pentad mean OLR data on 2.5° × 2.5° grids were derived from NOAA satellite observation (Gruber and Krueger 1984) extending from 1975 to 1995 with 9 months of 1978 missing.

Climatological pentad means of wind, geopotential height, vertical *p*-velocity, temperature, and specific humidity at multiple levels were constructed from daily mean data of the National Centers for Environmental Prediction (NCEP) reanalysis during 1979–1995 (Kalnay et al. 1996). These data have a horizontal resolution of 2.5° × 2.5°. The skin temperature, surface heat fluxes, and wind at 10 m are on Gaussian grids of T62 with horizontal resolution of about 1.9° × 1.9°. Over the open ocean, the skin temperature is fixed at the Reynolds SST in the NCEP reanalysis (Kalnay et al. 1996).

3 The three abrupt changes of circulation

To document the three distinct stages of the onset, we examine the circulation changes around the onset. The important circulation systems for the WNPSM include the WNP subtropical high, the monsoon trough, and the upper-level South Asian anticyclone. Figure 2 shows the difference maps constructed by subtracting two-pentad means before the onset from those after the onset. In the following, we describe the circulation changes at the onset of the three stages, respectively.

At the onset of the SCS summer monsoon, concurrent with the large increase of the rain rate (Fig. 2c) are the height decreases at 500 hPa (Fig. 2a) and the

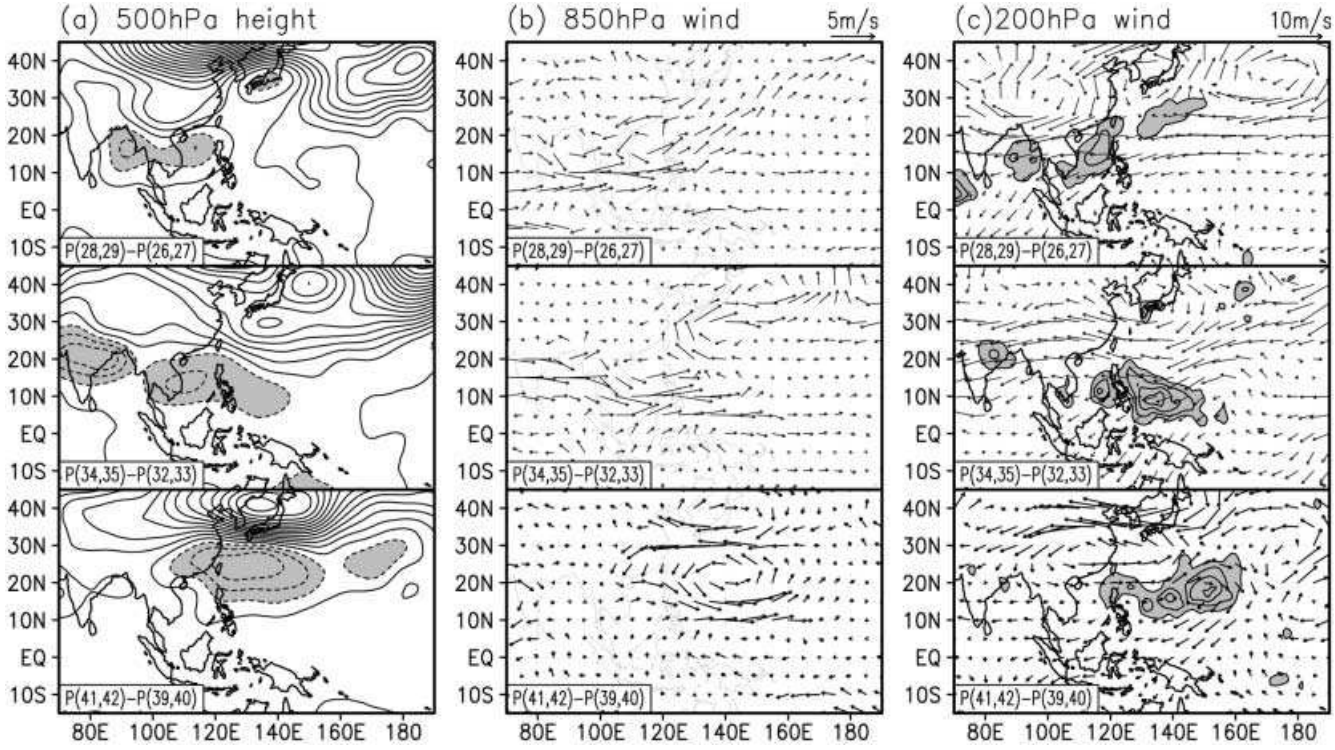

Fig. 2a–c Changes of climatological pentad mean **a** 500 hPa geopotential height (m), **b** 850 hPa wind, and **c** 200 hPa wind. From *top* to *bottom* are, respectively, pentad 28–29 minus pentad 26–27, pentad 34–35 minus pentad 32–33, and pentad 41–42 minus pentad 39–40. The contour interval in **a** is 4 m with the *shaded regions* denoting height changes less than −8 m. Contours in **c** denote rain rate changes over 3 mm/day (*shaded*) with an interval of 3 mm/day. The *wind scales* are indicated on the *top-right corner*

cyclonic wind changes at 850 hPa (Fig. 2b) over the SCS. The strong cyclonic wind changes over the SCS were indicated in previous studies (Wang and Wu 1997; Lau and Yang 1997; Yan 1997; Ueda and Yasunari 1998; Lau et al. 1998). Along the zonal band of 5°–10°N and from the Bay of Bengal to the SCS, the zonal winds at 850 hPa increase by about 4 m/s (Fig. 2b). These changes correspond to a sudden northeastward retreat of the WNP subtropical high from pentad 26 to pentad 27 (Fig. 3a) and the quick establishment of the monsoon trough over eastern SCS at pentad 28 (Fig. 3b), consistent with Lau and Yang (1997). At 200 hPa, a wide zonal band along 10°–25°N displays clear easterly tendencies (Fig. 2c). The anticyclonic wind development over the Tibetan Plateau reflects the northwestward displacement of the South Asian anticyclone. The increase of the upper-level divergence was indicated by the divergent wind changes over the SCS with intensified upper-level cross-equatorial northeasterly flow over the eastern Indian Ocean. Deep convection flares up suddenly over the SCS at pentad 28, as indicated by the sudden eastward shift of the 240 Wm^{-2} contour of OLR from the west coast of the SCS to the east of the Philippines between 10°–20°N (Fig. 3c).

At the onset of the second stage, the largest rain rate increase is found over the western Philippine Sea around 135°E and 10°N (Fig. 2c). Coherently, the pressure drops and the cyclonic winds strengthen over the SCS-WNP (Fig. 2a, b). A significant enhancement of westerlies is found over the SCS-Philippine Sea along 5°–15°N (Fig. 2b). The cross-equatorial lower-level southerlies increase clearly over the maritime continent. These changes reflect the northward lift of the subtropical high and the northeastward displacement of the monsoon trough. The 5880 m contour at 500 hPa displays a relatively quick northward shift from pentad 33 to pentad 34 (Fig. 3a). The monsoon trough shows large northeastward march during pentad 32–34, from the eastern SCS to the southwestern Philippine Sea (Fig. 3b). At 200 hPa, following the enhancement of easterlies along 20°–30°N and cross-equatorial northeasterlies over the maritime continent, strong divergence develops over the western Philippine Sea (Fig. 2c). The development of convection over the southwestern Philippine Sea is seen in the northeastward shift of the 240 Wm^{-2} contour of OLR (Fig. 3c).

At the onset of the third stage, a large increase of rainfall is found around 150°E and 17.5°N (Fig. 2c). The 500 hPa height change displays a strong dipole structure over the WNP and East Asia: the pressure falls over the subtropics (~25°N) and rises over the middle latitude (~40°N) (Fig. 2a). This feature is consistent with Ueda et al. (1995). Such a dipole structure is also present at 850 hPa and 200 hPa (Fig. 2b, c). The cyclonic-anticyclonic dipole tends to tilt northwestward with the altitude. The height decrease over the subtropical WNP signifies the weakening and eastward retreat of the WNP subtropical high. At pentad 42, the main part of the

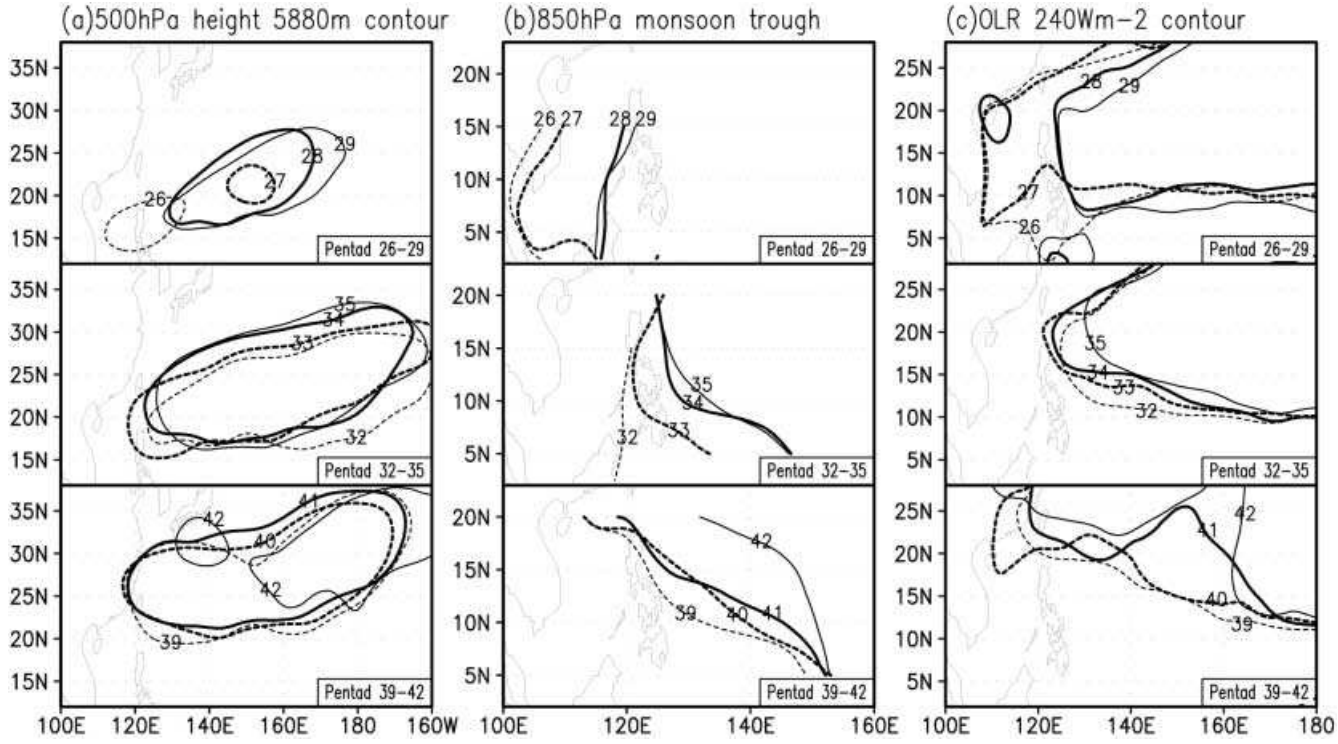

Fig. 3a–c The 5880 m contours of 500 hPa geopotential height, **b** locations of the 850 hPa monsoon trough, and **c** the 240 Wm^{-2} contours of OLR. From *top* to *bottom* are for, respectively, pentad 26–29, pentad 32–35, and pentad 39–42. The *labels* on the *contours* indicate the pentad. The data used are climatological pentad means

WNP subtropical high retreats eastward to the east of 150°E with a separate center formed to the southeast of Japan (Fig. 3a). The lower-level cyclonic wind change (Fig. 2b) corresponds to the quick northeastward shift of the monsoon trough observed at pentad 42 (Fig. 3b). The strengthening westerlies over the Philippine Sea connect with the intensifying cross-equatorial flow over Borneo and north of New Guinea (Fig. 2b). The 200 hPa wind change displays a clear anticyclone around 150°E and 17.5°N accompanied by enhanced cross-equatorial northeasterly flow around 145°E (Fig. 2c). The sudden development of convection in the northeastern part of the WNPSM domain is clearly indicated by the northeastward extension of the 240 Wm^{-2} contour of OLR (Fig. 3c).

The abrupt circulation changes at the onset of the three stages are remarkable. The observed pressure decrease, lower-level cyclonic wind change, and upper-level divergent flow region moves eastward or northeastward, in agreement with the onset advance. The lower-level cyclonic wind change is located to the northwest of the rain rate increase region, suggesting a Gill-type response of the circulation to the tropical heating (Gill 1980). On the other hand, the development of the upper-level divergent flow and the lower-level convergence can intensify the convection. The almost simultaneous changes in the convection and large-scale circulation suggest the role of the circulation-convection interaction in the abrupt onset of monsoon. The abruptness of the changes may indicate the presence of some kind of dynamic instability and the role of multi-scale interaction (Lau and Yang 1997).

4 The role of the climatological ISO and seasonal cycle

The abruptness of the onset should be related to the atmospheric internal dynamics since the external forcing (solar radiation and SST forcing) changes slowly. In this section, we discuss how the multi-stage onset is associated with the climatological ISO and the slow seasonal evolution.

The predominant period of the climatological ISO is about 30 days in the WNP (Wang and Xu 1997). The time interval between the consecutive stages of the onset is also about one month. This suggests that the climatological ISO may play an important role in the multi-stage onset of the WNPSM. The times of the first stage onset in the SCS in mid-May and the second stage onset in the southwestern Philippine Sea in mid-June all coincide with the arrival of a wet phase of the climatological ISO (Wang and Xu 1997). The onset in late-July in the northeastern part of the WNPSM domain is also the time when a wet phase of the climatological ISO develops locally.

However, the wet phase of the climatological ISO occupies a much larger zonal band than the onset region at the correspondent stage. For example, the wet phase of the climatological ISO in pentad 28 extends from the SCS to 150°E (Fig. 11a of Wang and Xu 1997 and

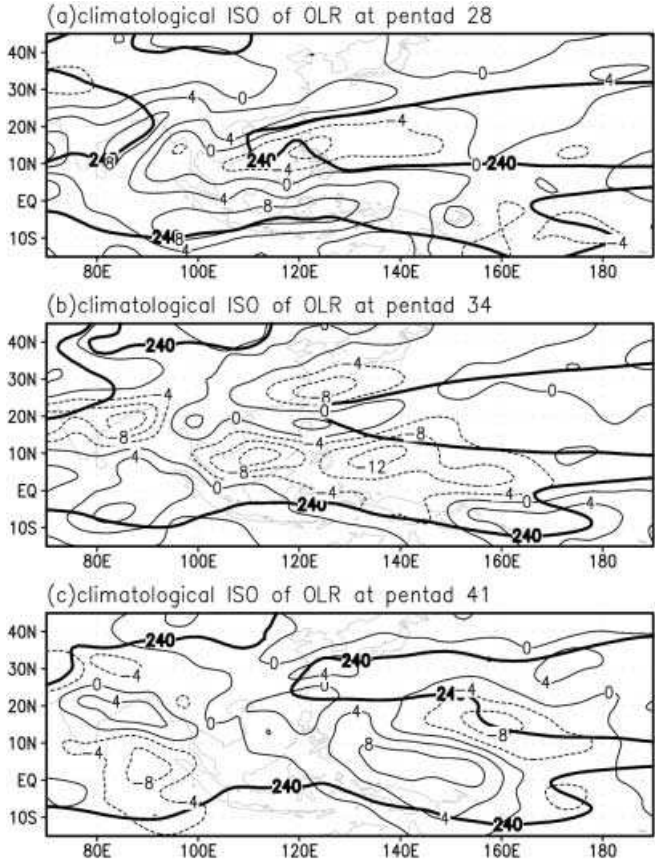

Fig. 4a–c Climatological ISO of pentad mean OLR **a** at pentad 28, **b** pentad 34, and **c** pentad 41. The contour interval is 4 Wm^{-2}. The *thick contours* are for 240 Wm^{-2} of the OLR climatological seasonal cycle. Refer to the text for the details of the ISO and the seasonal cycle

Fig. 4a). Though the amplitude of the climatological ISO decreases toward the east of the Philippines, this alone cannot explain why the onset does not occur over the Philippine Sea at pentad 28. A similar situation occurs at pentad 34 (Fig. 12a of Wang and Xu 1997 and Fig. 4b). An important factor to be considered here is the seasonal march. To clarify this point, we show in Fig. 4 the climatological ISO of OLR at pentad 28, 34, and 41 that represent, respectively, the first, second, and third stage of the onset. The ISO component is represented by the sum of the Fourier harmonics with periods of 20–72 days. Superposed on Fig. 4 are the 240 Wm^{-2} contours of the OLR climatological seasonal cycle (represented by the annual mean and the first four annual harmonics with periods of 90 days and longer). These contours are used to distinguish the wet and dry periods of the seasonal cycle (here, we use the "wet period" for the seasonal cycle to distinguish it from the "wet phase" for the climatological ISO).

At pentad 28, although the wet phase of the climatological ISO extends to the Philippine Sea, the seasonal cycle in the Philippine Sea is well before its transition to the wet period (Fig. 4a). In contrast, the seasonal cycle at the SCS is in or about to transit into the wet period. Around mid-June (pentad 34), another wet phase of the climatological ISO from the equatorial region arrives at the SCS and WNP (Wang and Xu 1997 and Fig. 4b). This wet phase extends from the SCS to the east of 150°E. At this time, the seasonal cycle is close to its transition phase in the western Philippine Sea. Thus, rainy season starts in the southwestern Philippine Sea. In the northeastern part of the WNPSM domain, the seasonal cycle remains in the dry period and no onset occurs. After mid-July (pentad 41), a third wet phase of the climatological ISO develops around 15°N and 160°E and extends westward (Fig. 4c). At this time, the seasonal cycle advances to the transition period in the northeastern part of WNPSM domain. As a result, the onset finally extends to the entire WNPSM domain.

From this discussion, the onset occurs when a wet phase of the climatological ISO arrives or develops. However, this condition alone is insufficient to warrant the onset. For the onset to occur, the seasonal cycle must march to a transition stage. Thus, the step wise northeastward advance of the onset over the WNPSM domain is due to a cooperative contribution of the seasonal cycle and the climatological ISO. The seasonal evolution establishes a favorable large-scale circulation and thermodynamic condition. It also regulates the amplitude and propagation of the ISO, resulting in the phase-lock of the ISO to the seasonal cycle. Because the seasonal transition takes about two months to cross the WNPSM domain (Fig. 4, Fig. 4a of Wang 1994) and the dominant period of the climatological ISO over the WNP is about one month (Wang and Xu 1997), the onset over the WNPSM domain exhibits three distinct stages.

5 The eastward progress of the seasonal cycle

The slow eastward progress of the seasonal cycle determines the direction for the advance of the WNPSM onset. Climatologically, the monsoon trough marches eastward and northeastward during May–July. This is consistent with the eastward progress of low-level westerlies along 5°–15°N over the SCS and WNP (Fig. 2b). The eastward shift of 200 hPa divergent winds indicates that the upper-level divergence moves eastward with season (Fig. 2c). The easterly shear zone obviously progresses eastward along 10°–20°N (Fig. 5a). The zone of high convective instability also extends eastward (Fig. 5c). The eastward extension of the upper-level divergence, the easterly vertical shear, and the high convective instability zone along with the eastward moving monsoon trough determines the seasonal progress of convection.

The eastward march of the monsoon trough and the high convective instability zone is related to the seasonal migration of the warm SST center in the SCS and the Philippine Sea, which will be discussed in the next section. The change of the vertical shear can be explained by the reversal of the meridional temperature gradient (Fig. 5b). The meridional temperature gradient averaged

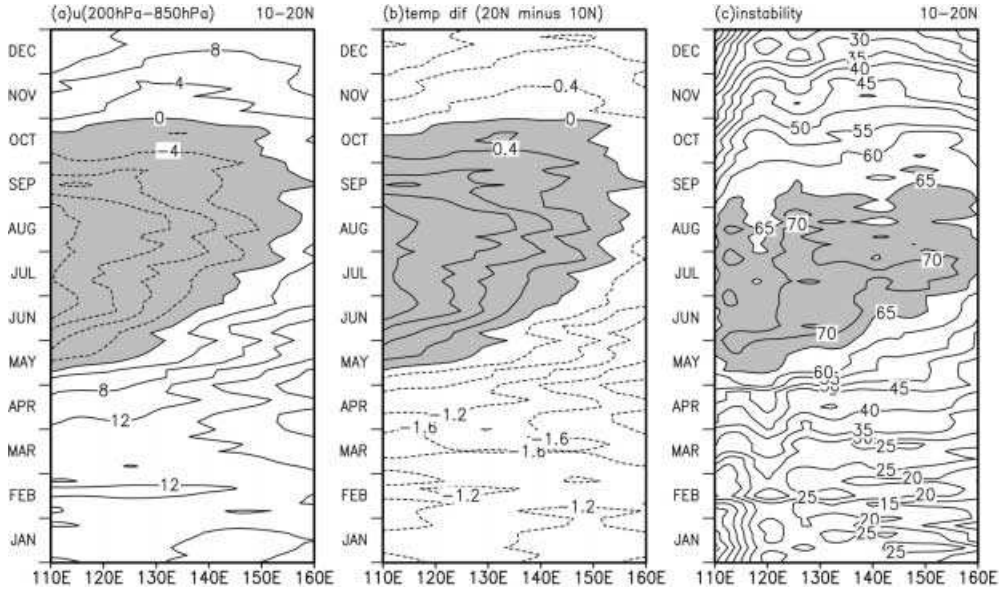

Fig. 5a–c Hovemöller diagrams of vertical shear of zonal wind (m/s) between **a** 200 hPa and 850 hPa averaged over 10°–20°N, **b** temperature difference (°C) between 20°N and 10°N averaged over the 850–200 hPa layer, and **c** instability index (K/1000 hPa) averaged over 10°–20°N. *Shading* in **a**, **b**, and **c** denotes, respectively, easterly vertical shear, positive temperature difference, and instability index over 65 K/1000 hPa. The instability index is defined as the difference of the saturated equivalent potential temperature between 1000 hPa and 700 hPa (divided by the pressure difference)

over the layer of 850–200 hPa reverses first over the Indochina Peninsula because the atmosphere heats up more quickly over the land than over the ocean. As a result, the easterly vertical shear develops first along southeast Asian longitudes.

To identify the mechanisms for the eastward progress of the southward temperature gradient, we diagnose the terms in the thermodynamic equation,

$$\partial T/\partial t = -V \cdot \nabla T - \omega\{\partial T/\partial p - RT/(C_p P)\} + Q_1/C_p$$

In this formula, T is the temperature, **V** the horizontal velocity, ω the vertical p-velocity, and p the pressure. Q_1 is the apparent heat source (Yanai et al. 1973). R and C_p are, respectively, the gas constant and the specific heat of dry air. Term Q_1 is calculated for each pressure level using the central difference scheme except for the lowest and topmost levels at which the finite difference is derived from the closest two levels. The thermodynamic equation interprets the local time change of temperature in terms of horizontal advection, adiabatic and diabatic heating.

The reversal of the meridional temperature gradient between 20°N and 10°N is mainly due to the temperature increase at the subtropical side since the local change rate of temperature is small at the tropical side. Figure 6 presents Hovemöller diagrams of different terms in the thermodynamic equation along 20°–25°N. The two dominant terms (the adiabatic and diabatic heating) are of opposite sign. Thus, we show their net effect (Fig. 6c). After January, the local change rate is dominated by positive values (Fig. 6a). This is attributed to the horizontal advection between 110°–120°E (Fig. 6b), the net effect of the adiabatic and diabatic heating east of 145°E (Fig. 6c), and both between 120°–145°E. East of 120°E, the adiabatic warming is maintained till about one month before the reversal of the meridional temperature gradient (Fig. 6d). After that, the diabatic heating becomes positive (Fig. 6e). Since the reversal of the temperature gradient is a process of temperature change for a few months, it is inferred that the horizontal advection has a major contribution over the SCS. Over the WNP, the adiabatic heating becomes more important and east of 145°E it is the major reason for the reversal of the meridional temperature gradient. The diabatic heating in relation to the spring rainfall in southern China and subtropical WNP makes a positive contribution from about one month before the monsoon onset.

Following the warming up over the land, an eastward temperature gradient is established over the subtropical East Asia and WNP at upper-levels. At lower-levels, strong northward or northeastward temperature gradient is present along the East Asian coast. Before the onset of the WNPSM, westerlies prevail at upper-levels and lower-level southwesterlies exist to the northwest flank of the WNP subtropical high. Thus, the horizontal advection is positive along the southeast China coast. Over the subtropical WNP (~20°N), there is downward motion that is linked to the ascent of the ITCZ and the spring rainfall over South China through to the south of Japan. As a result, there is adiabatic warming. Through the horizontal advection and the adiabatic warming (Fig. 6), the tropospheric warming extends eastward, resulting in the eastward extension of the southward temperature gradient and the easterly vertical shear (Fig. 5). The established easterly vertical shear, along with the increase of the convective instability, remarkably enhances the emanation and development of the Rossby waves in the WNP (Wang and Xie 1997), thus sustaining the ISO in the WNPSM domain.

6 The role of the seasonal SST change

Though the sudden onset is related to the atmospheric internal dynamics, the eastward seasonal progress is a

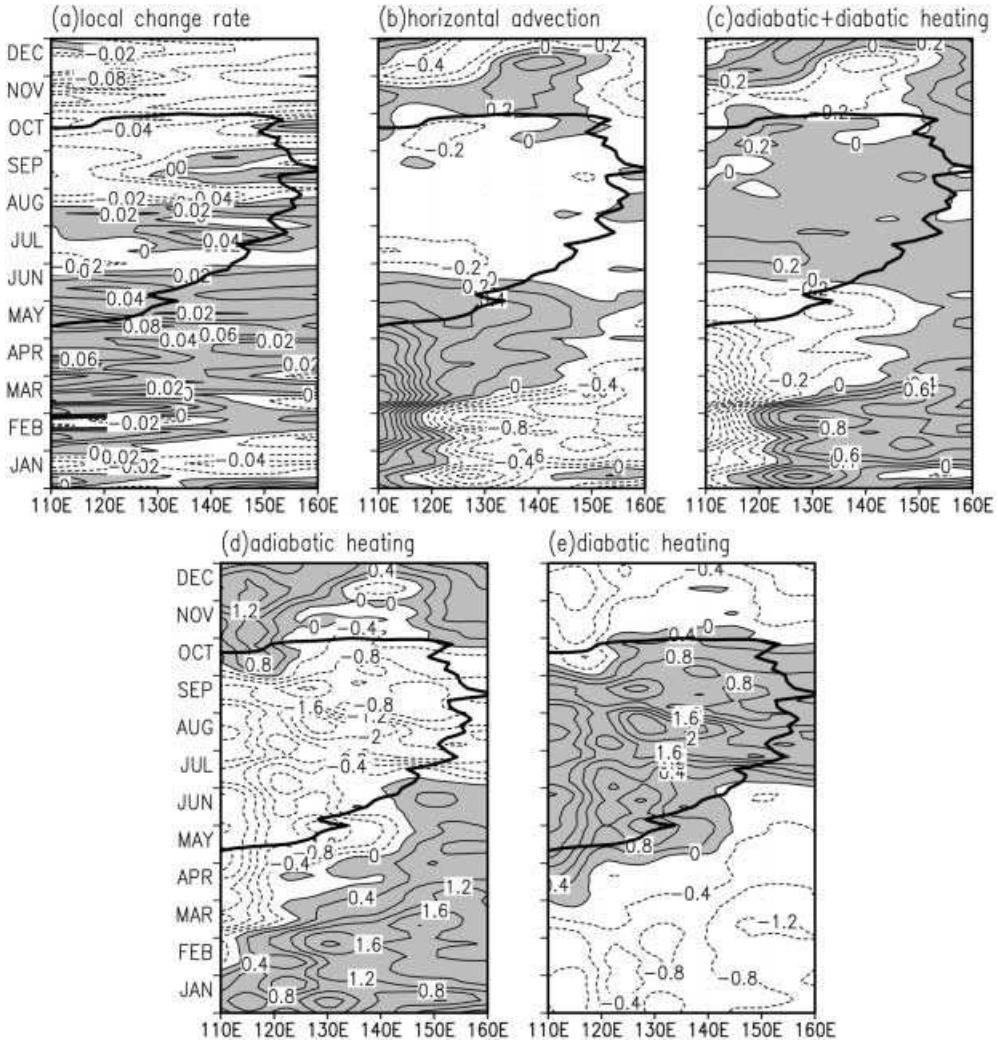

Fig. 6a–e Hovemöller diagrams of **a** the local change rate of temperature, **b** horizontal advection, **c** sum of the adiabatic and diabatic heating, **d** adiabatic heating, and **e** diabatic heating along 20°–25°N averaged over the layer of 850–200 hPa. The contour interval is 0.02 K/day in **a**, 0.2 K/day in **b** and **c**, and 0.4 K/day in **d** and **e**. The *thick contours* denote the time when the temperature difference between 20°N and 10°N averaged over the 850–200 hPa layer reverses its sign (refer to Fig. 5b). For clarity of presentation, smoothing was applied in the plot

slow process that may be affected by the SST variation. In this section, we discuss the seasonal SST change in the SCS and WNP and its plausible role in the northeastward march of the onset.

6.1 The seasonal SST change

In the central SCS, the SST exceeds 29.5 °C after pentad 24 (Fig. 7a). The extent of the 29.5 °C contour in the SCS expands from pentad 24 to pentad 26, which leads the SCS monsoon onset. Thereafter, the 29.5 °C contour shows little change of extent during pentad 27–33 (Fig. 7a, b). It begins to shrink quickly after pentad 34 (Fig. 7b). The high SST region in the equatorial western Pacific extends northwestward to the Philippine Sea at pentad 29 (Fig. 7a). A new center of SST over 29.5 °C forms to the east of Philippines after pentad 30 (Fig. 7b), a few pentads before the onset in the southwestern Philippine Sea. This new center of high SST intensifies and the warm SST tongue extends northeastward continuously from pentad 31 to pentad 37. At the same time, the SST in the equatorial western Pacific decreases. From pentad 38 to pentad 40, a high SST band is maintained between 15–20°N with an eastward bound being located around 145°E (Fig. 7c). The eastward bound extends quickly to around 148°E at pentad 41, concurrent with the onset of the third stage.

To understand the seasonal SST change, we display in Fig. 8 Hovemöller diagrams of pentad mean SST tendency, shortwave radiation, latent heat flux, and surface wind speed along a diagonal from 5°N and 95°E to 25°N and 175°E. This diagonal is selected based on the northeastward migration of the warmest SST. The large SST tendency in the SCS (105°–120°E) during February through early May (Fig. 8a) is associated with strong short wave radiation (Fig. 8b), weak latent heat flux (Fig. 8c) and oceanic mixing due to the low wind speed (Fig. 8d). The large SST tendency allows the development of the high SST center in the SCS before the onset over the SCS (Fig. 7a).

After mid-May (pentad 28), the SST in the SCS begins to decrease (Fig. 8a) following the SCS monsoon onset due to the cloud blocking of solar radiation (Fig. 8b) and the increase of latent heat flux (after May) (Fig. 8c) and oceanic mixing in association with the

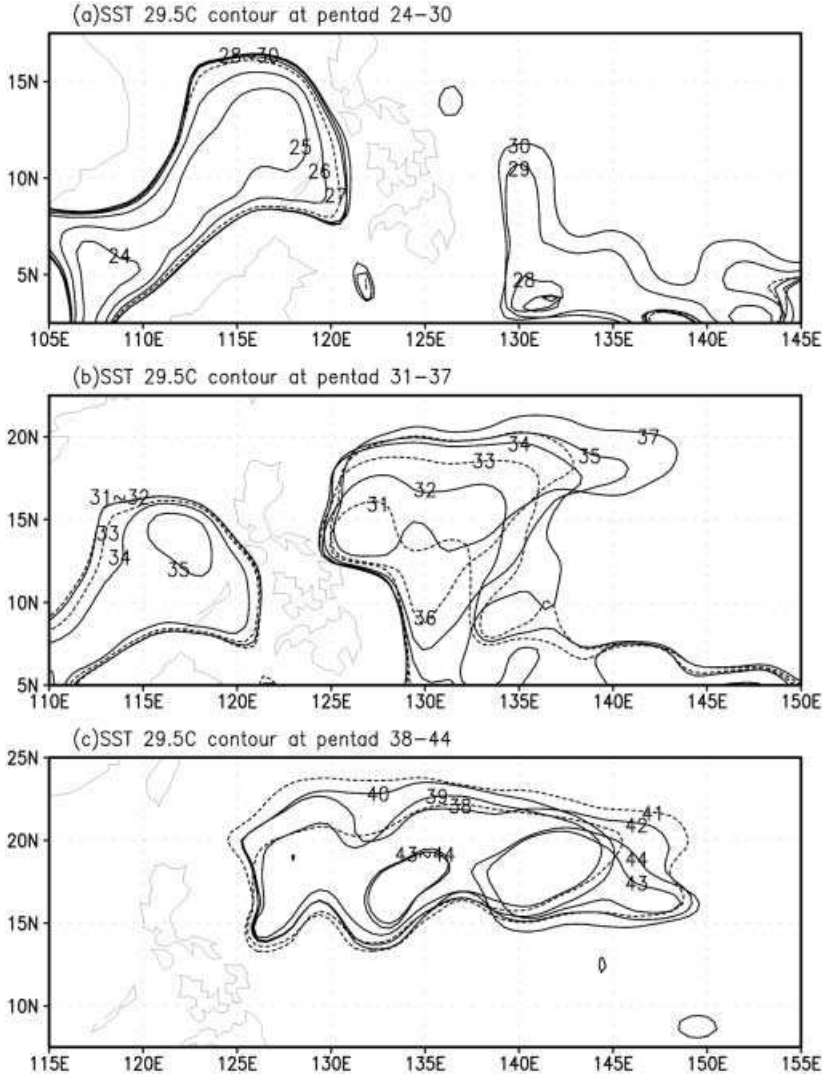

Fig. 7a–c Contours of climatological pentad mean SST at 29.5 °C for **a** pentad 24–30, **b** pentad 31–37, and **c** pentad 38–44. The *labels* on the *contours* indicate the pentad

enhancement of wind speed (Fig. 8d). On the other hand, the SST in the western Philippine Sea (120°–140°E) keeps rising from mid-May to mid-June. Around mid-June (pentad 33), the SST in the western Philippine Sea becomes higher than in the SCS so that the western Philippine Sea becomes the warmest center before the onset over the southwestern Philippine Sea (Fig. 7b).

Following the onset in mid-June, the SST in the western Philippine Sea (125°–140°E) begins to decrease (Fig. 8a) due to the cloud blocking of solar radiation (Fig. 8b). However, east of 140°E, the SST still rises from mid-June to mid-July due to high solar radiation and small amounts of oceanic mixing in relation to the decrease of wind speed. After mid-July, the SST east of 140°E becomes the highest (Fig. 7c), which is followed by the third stage onset in the northeastern part of the WNPSM domain.

After March, the SST in the SCS region becomes higher than the surrounding land regions and the Philippine Sea (Fig. 7a). Because the land surface temperature to the west changes little in April and May and the rate of SST increase in the Philippine Sea is smaller than in the SCS (Fig. 8a), the thermal contrast (with the warmest center in the SCS) increases until mid-May when the onset occurs in the SCS. After mid-May, the thermal contrast between the SCS and the Philippine Sea decreases. The temperature gradient reverses around mid-June (Fig. 7b) so that the western Philippine Sea becomes the warmest center. After mid-June, with the eastward extension of the high SST tongue along 15°–20°N and the decrease of SST in the western Philippine Sea, a new warmest center develops east of 140°E around late-July (Fig. 7c). Thus, with the seasonal change of SST, the high SST center moves from the SCS before mid-May to the western Philippine Sea around mid-June, and to the eastern Philippine Sea after mid-July.

6.2 The role of the seasonal SST change

The development of the high SST center can increase the surface air temperature and humidity through enhancing surface heat fluxes. This favors the increase of the

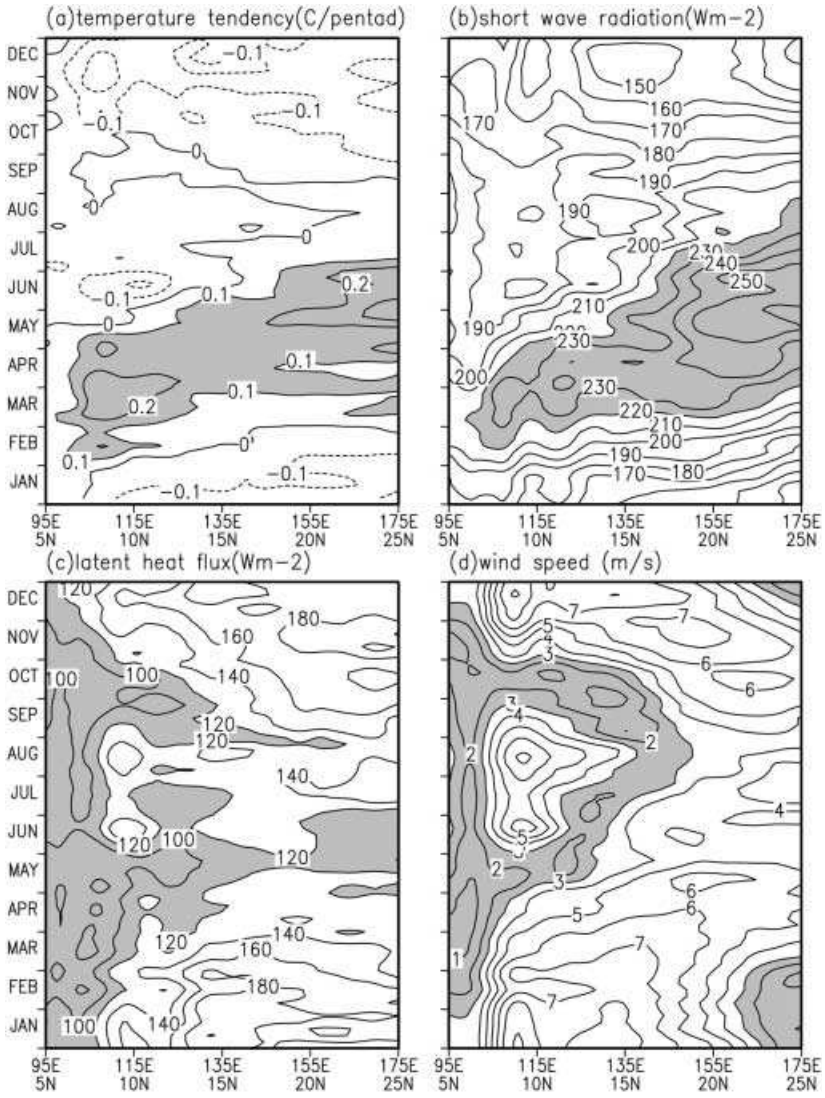

Fig. 8a–d Hovemöller diagrams along a diagonal from 5°N and 95°E to 25°N and 175°E for climatological pentad mean ocean (land) surface **a** temperature tendency (°C/pentad), **b** surface short wave radiation (Wm^{-2}), **c** latent heat flux (Wm^{-2}), and **d** wind speed at 10 m (m/s). Shading in **a**, **b**, **c**, and **d** denotes, respectively, surface temperature tendency over 0.1 °C/pentad, short wave radiation over 220 Wm^{-2}, latent heat flux below 120 Wm^{-2}, and wind speed below 3 m/s. For clarity of presentation, smoothing was applied in the plot

convective instability. Figure 9 shows the change of an instability index defined as the difference of saturated equivalent potential temperature between 1000 hPa and 700 hPa (divided by the pressure difference). The contour of 72 K/1000 hPa was chosen subjectively to illustrate the movement of the high instability region. A high instability region develops rapidly over the SCS during pentad 25–28 (Fig. 9a). From pentad 28 to pentad 30, the high instability region remains to be confined to the SCS. From pentad 31 to pentad 34, the high instability region extends quickly northeastward to around 135°E (Fig. 9b). During pentad 35–38, the eastward bound of the high instability region shows little change north of 10°N. After pentad 38, a high instability tongue develops between 15°–20°N and 135°–155°E (Fig. 9c). This high instability tongue weakens and disappears after pentad 41. Comparison of Figs. 7 and 9 indicates a good relation between the instability increase and the local SST warming. For example, an abrupt increase is found in both SST and instability before the onset in the SCS. Pentad 28–31 is a period without significant changes in the SCS. During pentad 32–34, both high SST and instability develop and extend northeastward to the western Philippine Sea. Comparison of area-mean SST and instability tendencies indicates that when the SST increases, the instability increases accordingly although the instability tendency contains higher frequency fluctuations.

The development of the warm SST center decreases local pressure which, in turn, induces low-level convergence. For example, the monsoon trough forms over the eastern SCS at pentad 28 (Fig. 3b), a few pentads after the SST exceeds 29.5 °C in the SCS (Fig. 7a). The monsoon trough marches to the western Philippine Sea at pentad 34 (Fig. 3b), following the development of the warmest SST tongue there (Fig. 7b). The sudden northeastward displacement of the monsoon trough from pentad 41 to pentad 42 (Fig. 3b) is observed after the extension of the warmest SST tongue to the east of 145°E at pentad 38 (Fig. 7c). This relation suggests that the acceleration of the monsoon westerlies to the southwest of the high SST center may be associated with

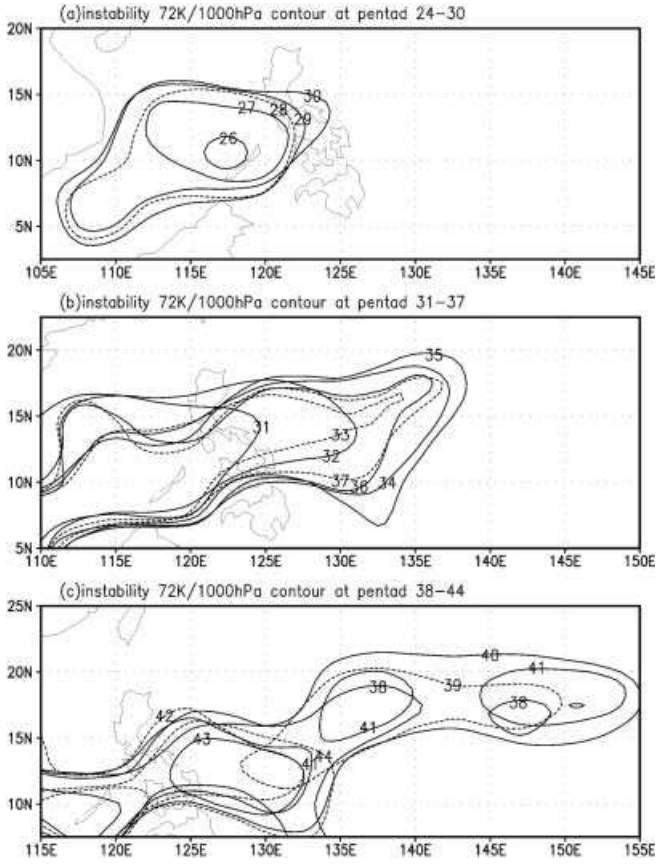

Fig. 9a–c Similar to Fig. 7 but for the instability index at 72 K/1000 hPa

the establishment of the SST gradient. However, the relationship is not perfect. The instability depends also on the middle-level air temperature change that may have little to do with the local SST change. The boundary layer air temperature and humidity changes also depend on the horizontal advection that is not solely determined by the SST gradient. The low-level convergence depends, in part, on the large-scale circulation changes which are related to the thermal contrast in a much larger spatial scale (e.g., Pacific basin-wide SST change and large-scale land-sea thermal contrast).

7 Summary and discussion

7.1 The SST effects

In the Indian monsoon region, the monsoon onset progresses northwestward (e.g., Indian Meteorological Department 1943). In Indonesia and northern Australia, the monsoon onset progresses southeastward (e.g., Murakami and Matsumoto 1994). The onset advance in those regions can be explained by the seasonal movement of solar radiation and the land-sea distribution. Because of the asymmetry of the land distribution about the equator in the Asian-western Pacific sector, the land heating effect induces a southeast-northwest march of convection (Meehl 1987). In the WNP, however, the onset of the monsoon rain marches northeastward, in accord with the eastward progress of the monsoon trough, the high convective instability region, the upper-level divergence, and the easterly vertical shear. Those, in turn, seem to follow the northeastward migration of the warm SST tongue in the WNP. Thus, we speculated that the seasonal SST change plays an important role in the northeastward progress of the rainy season in the WNP.

With the northeastward migration of high SST in the SCS and WNP, the thermal contrast changes with the warm center developing in the SCS before mid-May and in the Philippine Sea after mid-May. The related thermal contrast induces low-level moisture convergence and results in the increase of the low-level moisture and the convective instability. The westerlies are accelerated to the southwest of the warm SST center. Those changes favor the northeastward march of the monsoon trough and the high convective instability zone.

7.2 The role of the land-sea thermal contrast

An important feature at the summer monsoon onset is the switch of wind from easterly to westerly at lower-levels and from westerly to easterly at upper-levels (e.g., Murakami and Matsumoto 1994). The role of the reversal of the meridional temperature gradient in the establishment of the monsoon circulation has been discussed in previous studies (Flohn 1957; He et al. 1987; Li and Yanai 1996). Some studies (He et al. 1987; Yanai et al. 1992; Li and Yanai 1996) suggested the role of the sensible heat flux over the elevated Tibetan Plateau in the tropospheric warming over the Asian Continent during May-June. Recently, Hsu et al. (1999) indicated that the latent heat release over the sloping terrain south of the Tibetan Plateau and over the warm SST in the Bay of Bengal could be more influential. Using numerical experiments with prescribed diabatic heat source, Ose (1998) demonstrated the role of the broad-scale warming over the Eurasian continent centered around 25°N and 90°E.

From the temporal evolution of the terms in the thermodynamic equation (Fig. 6), the reason for the temperature increase varies with time and differs between the SCS and WNP. Over the SCS longitude, the temperature increase at the subtropical side is due to the horizontal advection and the adiabatic warming before March and the horizontal advection and the diabatic heating after March. The diabatic warming is due to the latent heat release in relation to the spring rainfall in southern China. The contribution of the horizontal advection to the temperature increase over the South China Plain was indicated by He et al. (1987). The positive horizontal advection is caused by the eastward advection of the warm air from the Tibetan Plateau and the Indochina Peninsula in relation to the westerly winds at middle and upper levels before the onset. In this sense,

the warming over the Tibetan Plateau due to the sensible heat flux contributes to the SCS monsoon onset. The latent heat flux over the sloping terrain south of the Tibetan Plateau becomes important only when the convection moves onto the southern slope of the Plateau. Thus, the establishment of the easterly vertical shear over the SCS is mainly due to the sensible heat flux over the Tibetan Plateau and the latent heat release over southern China and Indochina Peninsula. In the WNP, the adiabatic warming due to downward motion is more important and east of 145°E it plays the major role for the establishment of the easterly vertical shear along 10°–20°N.

The relative role of the land-sea thermal contrast and the SST change may differ between the SCS and WNP monsoon onset because of the difference of the geographic location. For the SCS monsoon onset, both the land-sea thermal contrast and SST change are important. Because the land lies right to the north of the SCS, the land-sea thermal contrast can affect the wind changes over the SCS through the change of the meridional temperature gradient. The role of the SST change can be felt through the surface heat fluxes and the turbulent mixing in the atmospheric boundary layer. These processes can modify the lower-level winds and the static stability. The SST effects are indicated in the development of the lower-level cyclonic vorticity (Fig. 2b) and the decrease of the static stability (Fig. 9a). For the WNP monsoon onset, due to the lack of geographically fixed land right to the north, the land-sea thermal contrast may play a less important role.

7.3 The combined role of the seasonal cycle and the ISO

The step wise advance of the onset is not unique to the WNP. In East Asia, the northward advance of the rain belt exhibits alternative stagnation and rapid northward movement (Lau and Li 1984; Lau et al. 1988; Tao and Chen 1987). Subbaramaya et al. (1984) indicated the presence of three stages of the onset in the Indian subcontinent. It remains to be demonstrated what are the formation processes for the step wise onset in East Asia and the Indian subcontinent. The relation between the seasonal progress and the ISO propagation shows differences among those regions. In the Indian monsoon region, the seasonal progress and the ISO propagation are both northwestward. Over the East Asian monsoon region, they are both northward. Over the WNP, the seasonal progress is mainly northeastward (Fig. 4a of Wang 1994) and the ISO propagates northwestward from the equator or develops locally (Lau and Chan 1986; Nitta 1987; Wang and Xu 1997). Though the ISO has a large zonal extent, the seasonal progress is gradual and the large-scale background is established first in the west and then in the east. Thus, the first onset occurs only in the west part where the seasonal cycle reaches its transition. The second onset in the middle occurs when a second wet phase of the climatological ISO arrives and at the same time the large-scale background transition is established. The third onset develops under similar conditions.

Though the climatological ISO is often the primary reason for the sudden onset, the onset is paced by the seasonal evolution of large-scale circulation and thermodynamics that determines the direction of the onset advance. The large-scale circulation and thermodynamic changes also control the occurrence and amplitude of the ISO. Wang and Xie (1997) demonstrated the importance of the vertical shear and the moisture availability for the development of the ISO in off-equatorial monsoon regions. Due to the establishment of the easterly vertical shear and the high convective instability over the SCS and WNP after April, the ISO is likely to propagate northward from the maritime continent or to develop locally in the WNP. With the large-scale background established by the seasonal evolution, the arrival of several one-after-another ISO wet phases triggers the development of deep convection. With the seasonal northeastward progress of the large-scale background and the dominant period of the ISO about 30 days in the WNP, the onset displays step wise northeastward advance with a time interval of about one month between the consecutive stages of the onset. The step wise march of the onset is observed each year. Due to the seasonal regulation, the ISO has a tendency to be phase-locked with respect to the calendar year so that the climatological onset displays multiple stages.

7.4 Interannual variation of the WNPSM onset

The three stages of the onset in the SCS and WNP are revealed based on climatological pentad mean data. The step wise feature of the onset advance is also clear in individual years. The domain and the time of each stage onset, however, change largely from year to year. In a relevant study (Wu and Wang 1999), we demonstrated that the interannual variation of the onset tends to be coherent in the WNPSM domain. Our observational and model studies showed that the SST anomalies in the tropical Pacific play an important role in the interannual variation of the WNPSM onset. The local SST anomalies in the WNP can induce large anomalies of the lower-level convergence and the convective instability. The warm SST anomalies in the equatorial central and eastern Pacific can cause significant changes in the upper-level circulation and large-scale vertical motion. These changes can impact significantly on the onset of the WNPSM. The detailed physical processes for the influence of ENSO on the interannual variation of the WNPSM onset were discussed in Wu and Wang (1999).

In this study, we focused on the changes in the tropics. Obvious changes also occur in East Asia. In particular, the wind and height changes in mid-June display a wave train structure along the East Asian coast (Fig. 2). Similar features were revealed in previous

studies (Ueda and Yasunari 1996, 1998; Ueda et al. 1995; Kawamura et al. 1996). This suggests that the heating in the tropics may induce circulation changes in the middle latitudes through Rossby wave propagation. In this sense, the seasonal evolutions over the WNP and East Asia may be connected. For example, the convection flare up in the southwestern Philippine Sea in mid-June excites a wave train from the Philippines to the North Pacific. The induced southwesterly winds over Japan may trigger the start of Baiu (rainy season in Japan) (Fig. 2). In late-July, the onset of convection in the WNP induces an anticyclone over Japan, leading to the commencement of the mid-summer dry weather in Japan, Korea, and the Yellow Sea (Nakazawa 1992).

Because the solar radiation reaching the ocean surface depends on the cloud amount and because the latent heat flux and the oceanic mixing rely on the surface wind changes, the seasonal SST variation is controlled by the monsoon. The decrease of SST after the onset indicates the feedback from the monsoon, mainly the reduction of solar radiation by cloud and the increase of latent heat flux and oceanic mixing induced by the enhanced wind speed. This indicates the importance of cloud-radiation and wind-evaporation feedbacks in the seasonal SST change and the northeastward migration of the warm SST pool in the SCS and WNP. Thus, the SST-monsoon relation is of interactive nature. This suggests that the northeastward march of the monsoon onset over the WNP is an interactive process. Further numerical modeling works are necessary and already underway.

Acknowledgements This study is supported by NSF Climate Dynamic Program, NOAA/OGP under GOALS and PACS Program, and ONR Marine Meteorology Program. The authors appreciate the comments from the two anonymous reviewers. This is the School of Ocean and Earth Science and Technology Publication 5086 and International Pacific Research Center Publication 43. The International Pacific Research Center is sponsored in part by the Frontier Research System for Global Change.

References

Chen T-C, Chen J-M (1995) An observational study of the South China Sea monsoon during the 1979 summer: onset and life cycle. Mon Weather Rev 123: 2295–2317

Flohn H (1957) Large-scale aspects of the "summer monsoon" in South and East Asia. J Meteorol Soc Japan 75th ann vol: 180–186

Gill AE (1980) Some simple solutions for heat-induced tropical circulation. Q J R Meteorol Soc 106: 447–462

Gruber A, Krueger AF (1984) The status of the NOAA outgoing longwave radiation data set. Bull Am Meteorol Soc 65: 958–962

He H-Y, McGinnis JW, Song Z-S, Yanai M (1987) Onset of the Asian summer monsoon in 1979 and the effects of the Tibetan Plateau. Mon Weather Rev 115: 1966–1995

Hendon HH, Liebmann B (1990) A composite study of onset of the Australian summer monsoon. J Atmos Sci 47: 2227–2240

Hsu H-H, Terng C-T, Chen C-T (1999) Evolution of large-scale circulation and heating during the first transition of Asian summer monsoon. J Clim 12: 793–810

Indian Meteorological Department (1943) Climatological atlas for airmen. Indian Meteorological Department, p 100

Kalnay E, Coauthors (1996) The NCEP/NCAR 40-year reanalysis project. Bull Am Meteorol Soc 77: 437–471

Kawamura R, Murakami T, Wang B (1996) Tropical and mid-latitude 45-day perturbations over the western Pacific during the northern summer. J Meteorol Soc Japan 74: 867–890

Lau K-M, Chan PH (1986) Aspects of the 40–50 day oscillation during the northern summer as inferred from outgoing longwave radiation. Mon Weather Rev 114: 1354–1367

Lau K-M, Li M-T (1984) The monsoon of East Asian and its global associations – a survey. Bull Am Meteorol Soc 65: 114–125

Lau K-M, Yang S (1997) Climatology and interannual variability of the southeast Asian summer monsoon. Adv Atmos Sci 14: 141–162

Lau K-M, Yang G-J, Shen S-H (1988) Seasonal and intraseasonal climatology of summer monsoon rainfall over East Asia. Mon Weather Rev 116: 18–37

Lau K-M, Wu H-T, Yang S (1998) Hydrological processes associated with the first transition of the Asian summer monsoon: a pilot study. Bull Am Meteorol Soc 79: 1871–1882

Li C, Yanai M (1996) The onset and interannual variability of the Asian summer monsoon in relation to land-sea thermal contrast. J Clim 9: 358–375

Meehl GA (1987) The annual cycle and interannual variability in the tropical Pacific and Indian Ocean regions. Mon Weather Rev 115: 27–50

Murakami T, Matsumoto J (1994) Summer monsoon over the Asian continent and western North Pacific. J Meteorol Soc Japan 72: 719–745

Murakami T, Chen L-X, Xie A (1986) Relationship among seasonal cycles, low-frequency oscillations, and transient disturbances as revealed from outgoing longwave radiation data. Mon Weather Rev 114: 1456–1465

Murakami T, Wang B, Lyons SW (1992) Contrasts between summer monsoons over the Bay of Bengal and the eastern North Pacific. J Meteorol Soc Japan 70: 191–210

Nakazawa T (1992) Seasonal phase lock of intraseasonal variation during the Asian summer monsoon. J Meteorol Soc Japan 70: 597–611

Nitta T (1987) Convective activities in the tropical western Pacific and their impacts on the Northern Hemisphere summer circulation. J Meteorol Soc Japan 65: 165–171

Ose T (1998) Seasonal change of Asian summer monsoon circulation and its heat source. J Meteorol Soc Japan 76: 1045–1063

Rasmusson EM, Arkin PA (1987) El Niño/Southern Oscillation and the Asian monsoon. In: Yeh, et al (eds) The climate of China and global climate. China Ocean Press, Beijing, pp 141–153

Soman MK, Kumar KK (1993) Space-time evolution of meteorological features associated with the onset of the Indian summer monsoon. Mon Weather Rev 121: 1177–1194

Subbaramayya IS, Babu V, Rao SS (1984) Onset of the summer monsoon over India and its variability. Meteorol Mag 113: 127–135

Tanaka M (1992) Intraseasonal oscillation and the onset and retreat dates of the summer monsoon over East, Southeast Asia and the western Pacific region using GMS high cloud amount data. J Meteorol Soc Japan 70: 613–629

Tao S-Y, Chen L-X (1987) A review of recent research on the East Asian summer monsoon in China. In: Chang C-P, Krishnamurti TN (eds) Monsoon meteorology. Oxford University Press, New York, pp 60–92

Ueda H, Yasunari T (1996) Maturing process of the summer monsoon over the western North Pacific – a coupled ocean/atmosphere system. J Meteorol Soc Japan 74: 493–508

Ueda H, Yasunari T (1998) Role of warming over the Tibetan Plateau in early onset of the summer monsoon over the Bay of Bengal and the South China Sea. J Meteorol Soc Japan 76: 1–12

Ueda H, Yasunari T, Kawamura R (1995) Abrupt seasonal changes of large-scale convective activity over the western Pacific in the northern summer. J Meteorol Soc Japan 73: 795–809

Wang B (1994) Climatic regimes of tropical convection and rainfall. J Clim 7: 1109–1118
Wang B, Wu R (1997) Peculiar temporal structure of the South China Sea summer monsoon. Adv Atmos Sci 14: 177–194
Wang B, Xie X (1997) A model for the boreal summer intraseasonal oscillation. J Atmos Sci 54: 72–86
Wang B, Xu X (1997) Northern Hemispheric summer monsoon singularities and climatological intraseasonal oscillation. J Clim 10: 1071–1085
Wang B, Wu R, Fu X (1999) Pacific-East Asian teleconnection: How does ENSO affect the East Asian climate? J Clim (in press)
Wu R, Wang B (1999) Interannual variability of summer monsoon onset over the western North Pacific and the underlying processes. J Clim (in press)
Xie P, Arkin PA (1997) Global precipitation: A 17-year monthly analysis based on gauge observations, satellite estimates, and numerical model outputs. Bull Am Meteorol Soc 78: 2539–2558
Yan J-Y (1997) Observational study on the onset of the South China Sea southwest monsoon. Adv Atmos Sci 14: 277–287
Yanai M, Li C, Song Z-S (1992) Seasonal heating of the Tibetan Plateau and its effects on the evolution of the Asian summer monsoon. J Meteorol Soc Japan 70: 319–351
Yanai M, Tomita T (1998) Seasonal and interannual variability of atmospheric heat sources and moisture sinks as determined from NCEP-NCAR reanalysis. J Clim 11: 463–482
Yanai M, Esbensen S, Chu J-H (1973) Determination of bulk properties of tropical cloud clusters from large-scale heat and moisture budgets. J Atmos Sci 30: 611–627